Precision Microwave Measurement of the $2\,^3P_1$-$2\,^3P_2$ Interval in Atomic Helium

C. H. Storry, M. C. George, and E. A. Hessels
Department of Physics, York University, 4700 Keele Street, Toronto, Ontario, Canada M3J 1P3
(Received 15 December 1999)

The $2\,^3P_1$-to-$2\,^3P_2$ interval in atomic helium is measured using a thermal beam of metastable helium atoms excited to the $2\,^3P$ state using a 1.08-μm diode laser. The $2\,^3P_1$-to-$2\,^3P_2$ transition is driven by 2.29-GHz microwaves in a coaxial transmission line. Our result of $2\,291\,174.0 \pm 1.4$ kHz is the most precise measurement of helium $2\,^3P$ fine structure. This measurement plays a key role in obtaining a new value for the fine-structure constant.

PACS numbers: 32.30.Bv, 31.30.Jv

Because of its long lifetime (98 ns) and large energy intervals (2.29 and 29.6 GHz), helium $2\,^3P$ fine structure has long been considered an excellent system in which to test QED and to measure the fine-structure constant α. Recently, Drake has calculated this structure to a precision of 20 kHz and is expected to present sub-kHz theoretical calculations soon [1,2]. A 1-kHz comparison between theory and experiment of the 29.6-GHz interval would lead to a 17 ppb (parts per 10^9) determination of α. In order to trust this value of α, it is vital to have a precise test of the QED calculations of the $2\,^3P$ structure. Fortunately, the 2.29-GHz interval allows for just such a precise test. The QED contributions for this interval are as large as those for the 29.6-GHz interval, but because it is 13 times smaller, a precise value of α is not necessary for a 1-kHz calculation. Thus, a measurement of the 2.29-GHz interval at the kHz level of precision tests the QED theory necessary to obtain a 17-ppb determination of α.

Current determinations of α obtained from the anomalous magnetic moment of the electron ($g - 2$) [3,4], from the quantum-Hall effect [5], from the ac-Josephson effect [6], and from measuring neutron de Broglie wavelengths [7] range in precision from 4 to 60 ppb but differ by as much as 250 ppb. A new 17-ppb measurement would be the second-most-precise determination of α and would shed light on the present discrepancies. Since $g - 2$ provides the most precise test of QED in any system, and since the precision of this test is limited by the precision of α, this new determination of α will lead to a stronger test of QED.

Presented here is a 1.4-kHz measurement [8] of the $2\,^3P_1$-to-$2\,^3P_2$ fine-structure interval. A schematic of the experiment is shown in Fig. 1. An intense thermal beam of $2\,^3S_1$ metastable He atoms is created in the dc-discharge source of Ref. [9]. It enters a region with a small vertical dc magnetic field B_z, which lifts the degeneracy of m substates. A circularly polarized (σ^+) 1.08-μm diode laser (A in Fig. 1) repeatedly drives $2\,^3S_1\,m$ atoms to the $2\,^3P_1\,m+1$ states, thus optically pumping the atoms into the $2\,^3S_1\,m = +1$ state. A second diode laser (B in Fig. 1), this one linearly polarized in the z direction, repeatedly drives $2\,^3S_1\,m = 0$ atoms up to the $2\,^3P_0\,m = 0$ state, thus emptying the $2\,^3S_1\,m = 0$ state of any residual population.

A third 1.08-μm laser (C in Fig. 1) is σ^- and is focused using a cylindrical lens to 20 μm at the atomic beam. It drives the $2\,^3S_1\,m = +1$ population up to the $2\,^3P_1\,m = 0$ state. 80 μm after passing through this laser beam (40 ns at the 2 km/s average speed of the atoms), before many of the $2\,^3P_1$ atoms spontaneously decay, the atoms enter a 7-mm-diameter 50-Ω coaxial microwave transmission line (D in Fig. 1). Here, a 2.29-GHz vertical microwave magnetic field drives the $2\,^3P_1\,m = 0$-to-$2\,^3P_2\,m = 0$ magnetic-dipole transition. The 8.0-W power of these microwaves is well below saturation and has only ~2% efficiency for driving this transition. Two-thirds of the resulting $2\,^3P_2\,m = 0$ atoms decay into the previously emptied $2\,^3S_1\,m = 0$ state. $2\,^3P_1\,m = 0$ atoms are forbidden from decaying into the $2\,^3S_1\,m = 0$ state due to a selection rule, and thus any repopulation of the $2\,^3S_1\,m = 0$ state is a direct indication that the 2.29-GHz transition has been driven. To detect these $2\,^3S_1\,m = 0$ atoms, a final laser (E in Fig. 1), linearly polarized in the z direction, excites the $2\,^3S_1\,m = 0$ atoms up to the $2\,^3P_0$ state. The resulting 1.08-μm fluorescence is focused onto a LN_2-cooled InGaAs photodiode. The frequencies of all four lasers are locked to saturated-absorption signals in rf-excited helium cells.

The atoms pass through the inner and outer conductors of the transmission line (D in Fig. 1) via 1.8-mm holes covered by thin conducting grids. Because the precision measurement occurs in the immediate vicinity, three

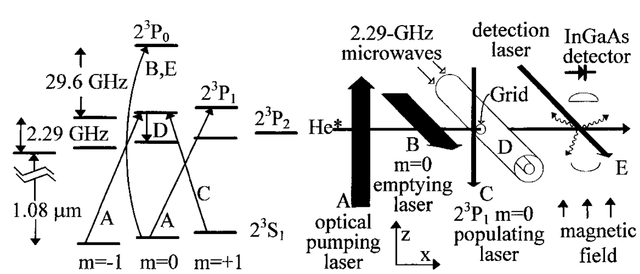

FIG. 1. Energy-level diagram and schematic of the experimental setup. Details are given in the text.

0031-9007/00/84(15)/3274(4)$15.00

different grids (20-μm-thick Cu with 7.5- and 19-μm square holes and 8-μm-thick Au with 10-μm square holes) are attached using two different silver paints to two distinct coaxial microwave regions in several distinct data runs to test for possible systematic effects.

The microwaves are 100% amplitude modulated and a lock-in amplifier is used to extract the photodiode signal synchronous with this modulation. This signal is averaged for typically 10 s at each of 37 microwave frequencies near the atomic resonance. More than 10 000 such scans are taken while varying a large variety of experimental parameters during several months of around-the-clock data collection. An average of data taken with typical experimental parameters is shown in Fig. 2.

The natural linewidth of the microwave resonance is 3252 kHz due to the 98-ns lifetime of both $2\,^3P$ states. The expected width is narrower since the amplitude of the microwave field increases (as $1/r$) as the atoms approach the center conductor of the coaxial region, causing longer-lived atoms to interact with a larger microwave field. Using time-dependent perturbation theory, this effect is modeled and the predicted width is 3029 kHz. Because of power broadening, the measured width at 8.0 W is 1.1 $\pm$ 0.1% broader than that at 5.3 W, indicating [10] that the 8.0-W resonance is power broadened by 3.3 $\pm$ 0.3% relative to zero power, thus predicting a width of 3128 $\pm$ 9 kHz at 8 W. Even with the grid covering it, a small fraction ($\sim$1 ppm) of the microwave power radiates out of the entrance hole. These radiated fields are phase shifted by $\sim$5° relative to those inside the region, causing a small Ramsey-separated-oscillatory-field effect which results in a slight narrowing and a shift of the resonance line shape as discussed in Ref. [9]. The narrowing is proportional to the time the $2\,^3P$ atoms spend in this radiated field and thus to the distance between laser C and the grid (see Fig. 1). By varying this distance from 80 to 330 μm, a narrowing of 0.05 $\pm$ 0.01 kHz/μm is observed, thus narrowing the linewidth to 3124 $\pm$ 9 kHz at 80 μm of separation. The average linewidth from Lorentzian fits of data taken with 8.0 W of microwave power and with an 80-μm separation is 3112 kHz, in reasonable agreement with this modeled width.

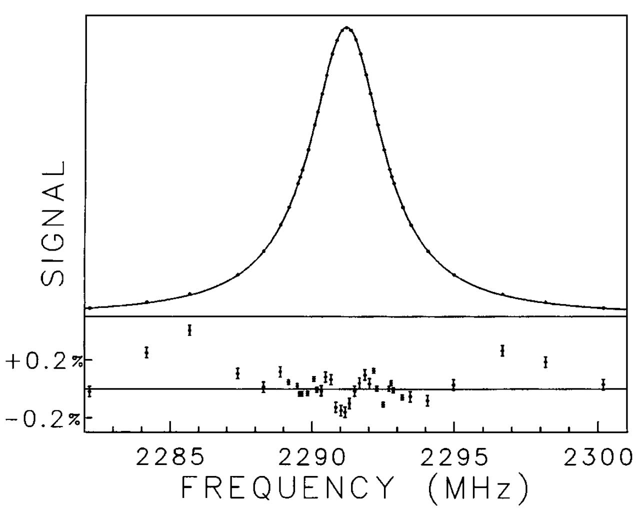

FIG. 2. Averaged data, Lorentzian fit, and residuals. Note the smaller error bars for the points near half maximum, which are repeated 5 times more often than the other points.

The expected line shape is Lorentzian [10] in the approximation that the microwave magnetic field is exactly vertical and constant in amplitude. The data points in Fig. 2 fit very well to a Lorentzian line shape. The small residuals (data points minus fit values) are shown at the bottom of Fig. 2. The largest residuals in this plot are small peaks at $\pm$6 MHz from the line center. These features result from atoms which undergo $2\,^3P_1\; m = 0$-to-$2\,^3P_2\; m = \pm 1$ microwave transitions in fields which are slightly nonvertical due to the curvature of the coaxial geometry near the top and bottom of the 1.8-mm entrance hole. The positions of these peaks are determined by the applied dc magnetic field (2.8 G), their widths are determined by the natural linewidth, and the observed heights of 0.3% agree with the heights modeled by averaging (over the cross section of the entrance hole) the effects due to these nonvertical fields. The residuals near the main resonance, away from the $\pm$6 MHz peaks, are small ($<$0.1% rms) and are approximately symmetric. When the small uncertainty in microwave power at each frequency is included, these residuals are consistent with a smooth symmetric curve which is slightly negative at line center and slightly positive at $\pm$1 MHz. The $1/r$ increase in amplitude of the microwave field and the sudden turn-off of the field as the atoms enter the inner conductor lead to a line shape which is slightly non-Lorentzian but still symmetric. This line shape has been modeled using time-dependent perturbation theory and yields residuals consistent with the pattern described above for the observed residuals.

Table I lists (in column 5) the average centers obtained from Lorentzian least-squares fits of data taken with the grids, microwave powers (P_μ), powers of laser C (P_L), and magnetic fields of columns 1–4. When combined, the centers give a net statistical uncertainty of $<$0.08 kHz. The final uncertainty in the measured line center is entirely dominated by systematic effects. The excellent signal-to-noise ratio in this measurement is used to test extensively these effects.

The shifts in the resonance due to the $\sim$1-ppm microwave power which radiates through the grid are also studied by varying the separation between laser C of Fig. 1 and the microwave region. When the laser is closer to the microwave region, the magnitude of this shift is small since the $2\,^3P$ atoms spend little time in the radiated field. Centers obtained with separations of 80 to 330 μm shift linearly with separation, with shift rates of 8.3 $\pm$ 4.5, 9.2 $\pm$ 5.2, and 2.4 $\pm$ 17.7 Hz/μm for the Cu 7.5-μm, Cu 19-μm, and Au 10-μm grids, respectively. The centers of column 5 are taken with an 80 $\pm$ 25-μm separation and corrections due to this separation are shown in column 6. A large uncertainty is included to allow for the possibility that the shifts are not linear for separations of $<$80 μm.

TABLE I. Summary of systematic effects and measured centers. The 1 standard deviation uncertainties in the last digits are given in parentheses.

Grid type	P_μ (W)	P_L (mW)	B field (G)	Fit center (kHz)	Extrapolation (kHz)	Zeeman shift (kHz)	Light shift (kHz)	Doppler shift (kHz)	Power slope (kHz)	Grid position (kHz)	Grid hole (kHz)	Measured center (kHz)
Cu	8.0	1	2.78	2 291 177.2(2)	0.7(7)	−4.1(2)	−0.1(1)	0.0(1)	−0.5(3)	0.6(6)	0.0(10)	2 291 173.8(14)
7.5 μm	8.0	1	5.42	2 291 188.5(3)	0.7(7)	−15.5(6)	−0.1(1)	0.0(1)	−0.5(3)	0.6(6)	0.0(10)	2 291 173.7(16)
	5.3	1	2.78	2 291 179.4(8)	0.7(7)	−4.1(2)	−0.1(1)	0.0(1)	−2.9(15)	0.6(6)	0.0(10)	2 291 173.6(22)
	8.0	10	2.78	2 291 178.4(4)	0.7(7)	−4.1(2)	−1.3(7)	0.0(1)	−0.5(3)	0.6(6)	0.0(10)	2 291 173.8(16)
Cu	8.0	1	2.78	2 291 177.6(2)	0.7(7)	−4.1(2)	−0.1(1)	0.0(1)	−0.5(3)	0.6(6)	0.0(10)	2 291 174.2(14)
19 μm	8.0	1	5.44	2 291 189.5(2)	0.7(7)	−15.6(6)	−0.1(1)	0.0(1)	−0.5(3)	0.6(6)	0.0(10)	2 291 174.6(15)
	5.3	1	2.78	2 291 180.4(5)	0.7(7)	−4.1(2)	−0.1(1)	0.0(1)	−2.9(15)	0.6(6)	0.0(10)	2 291 174.6(21)
	8.0	10	2.78	2 291 178.8(3)	0.7(7)	−4.1(2)	−1.3(7)	0.0(1)	−0.5(3)	0.6(6)	0.0(10)	2 291 174.2(16)
Au	8.0	1	2.80	2 291 177.9(5)	0.2(14)	−4.1(2)	−0.1(1)	0.0(1)	−0.5(3)	0.5(5)	0.0(10)	2 291 173.9(19)
10 μm	8.0	10	2.80	2 291 180.1(6)	0.2(14)	−4.1(2)	−1.3(7)	0.0(1)	−0.5(3)	0.5(5)	0.0(10)	2 291 174.9(20)

The largest systematic shift is due to the small 0.5283 $\mathrm{kHz/G^2}$ [11,12] quadratic Zeeman shift of the $2\,{}^3P_1\; m = 0$-to-$2\,{}^3P_2\; m = 0$ interval. The small magnetic fields applied in this experiment are measured to a precision of 2% using Hall-effect gaussmeters. The resulting Zeeman shift is listed in column 7.

A major concern in the experiment is the possible presence of laser fields where the microwave excitation occurs. Light shifts could result, and thus the grids are used to separate the microwave and laser fields. To test for small remaining light shifts, data are taken at both 1 and 10 mW of laser power in laser C. The 10-mW data are shifted by 1.14 ± 0.23 kHz from data at 1 mW, indicating a shift rate of 0.13 ± 0.03 kHz/mW.

The Doppler shift is <0.1 kHz since the microwave propagation is perpendicular (to within 6.5 mrad) to the atomic beam. The average vacuum pressure used in the experiment is 2×10^{-6} Torr. Some data are taken at higher pressure and, as expected, no shift of the line center is seen. The power shift (analogous to the ac Stark shift, but caused here by the microwave magnetic field) is calculated to be <0.01 kHz.

A Cs-clock-referenced (via a Global Positioning System receiver) source produces microwaves which are amplified and input to the coaxial microwave region. The variation of microwave power versus frequency is minimized by adjusting the input power to the amplifier at each frequency. The resulting output powers are measured several times during the experiment using a precision calorimeter [13]. The small shifts listed in column 10 are calculated by dividing the data points by the relative powers used at each frequency and refitting to determine the shifted line center. The 5.3-W data are taken with microwave powers which have larger variations versus frequency, and therefore larger corrections are listed in column 10. The agreement between the 5.3-W and 8.0-W final centers (see Table II) indicates that these corrections are well understood.

A verification of the calorimeter and gaussmeter measurements is obtained by reorienting the coaxial transmission line of Fig. 1 into the z direction, which allows the $2\,{}^3P_1\; m = 0$-to-$2\,{}^3P_2\; m = \pm 1$ transitions to be driven. The separation between these resonances is a measure of B_z. The relative heights of the $\Delta m = \pm 1$ resonances is a measure of the relative powers at their centers. Changing this separation by varying B_z allows for verification of the calorimeter measurements at several frequencies.

Variation of microwave power versus frequency can also result from small standing waves caused by reflections from the microwave region or the 50-Ω absorptive terminator. By careful microwave design, the reflected power is reduced to <25 ppm of the incident power, which results in a shift of <0.025 kHz. A test of standing-wave effects is made by reversing the orientation of the microwave region, which moves the interaction point by a quarter wavelength (see Table II).

The thin conducting grid over the entrance hole of the microwave region is displaced by $\sim 20\ \mu$m from the ideal coaxial geometry. This displacement is measured to an

TABLE II. Measured line centers with various experimental procedures. All values are given in kHz with 1 standard deviation uncertainties given in parentheses.

19-μm copper grid	2 291 174.2(14)
7.5-μm copper grid	2 291 173.8(14)
10-μm gold grid	2 291 173.9(19)
Conductive silver paint 1	2 291 174.0(15)
Conductive silver paint 2	2 291 174.2(14)
Magnetic field of 2.78 G	2 291 174.0(14)
Magnetic field of 5.43 G	2 291 174.2(16)
B field pointed upward	2 291 174.0(15)
B field pointed downward	2 291 174.1(14)
Microwave region 1	2 291 174.1(15)
Microwave region 2	2 291 173.8(15)
$+y$ orientation of microwave region	2 291 173.8(14)
$-y$ orientation of microwave region	2 291 174.2(15)
8.0-W microwave power	2 291 174.0(14)
5.3-W microwave power	2 291 174.3(21)
1-mW power for laser C	2 291 174.0(14)
10-mW power for laser C	2 291 174.0(16)
σ^+ polarization for laser C	2 291 174.0(15)
σ^- polarization for laser C	2 291 174.1(15)
Final measured result	2 291 174.0(14)

TABLE III. Previous measurements and theory of the $2\,^3P$ intervals. Values are in kHz with 1 standard deviation uncertainties.

	$2\,^3P_1$-to-$2\,^3P_2$	$2\,^3P_1$-to-$2\,^3P_0$
This work:	2 291 174.0 ± 1.4	
Previous measurements:		
Inguscio *et al.* [15]	2 291 174 ± 15	29 616 949.7 ± 2.0
Shiner *et al.* [14]	2 291 173 ± 3	29 616 962 ± 4
Wen and Gabrielse [16]	2 291 198 ± 8	29 616 936 ± 8
Hughes *et al.* [12]	2 291 196 ± 5	29 616 844 ± 21
Storry and Hessels [9]		29 616 966 ± 13
Theory		
Zhang and Drake [1]	2 291 180 ± 20	29 616 974 ± 20

accuracy of 1 μm by measuring the capacitive pickup on a probe which is inserted into the region and scanned over its surface. The displacement distorts the microwave fields near the grids. The effect of this distortion on the line center is studied by varying the position of the grid relative to the ideal geometry (from -350 to $+150$ μm). A very small shift of 0.035 ± 0.035 kHz per μm displacement is observed and a correction of this ratio times the measured displacement of each grid is included in column 11 of Table I.

The microwave fields in the coaxial transmission line are sustained by surface currents on the conductors. At the grid, these currents are forced to follow individual grid wires, thus slightly distorting the microwave fields in the vicinity. The size of this distortion and possible shifts of the resonance center depend on the size of the grid holes. The centers obtained with the three different grids are very consistent, varying by only ± 0.2 kHz. This consistency over the 7.5-μm-to-19-μm grid-hole size restricts possible extrapolations to zero grid-hole size to <1 kHz. In a second test for possible shifts due to grid-hole size, a small quantity of data is taken with much larger grid holes of 60 μm. These data also indicate that the three original grids give the correct center to within ~ 1 kHz.

Note that (for typical parameters) each of the systematic shifts of Table I is <0.7 kHz, except the easily calculated Zeeman shift, and this correction is directly confirmed by the consistency of measurements at different magnetic fields. The measured centers corrected for all systematic effects are shown in the final column. Table II shows the average centers obtained using a variety of experimental parameters. Note that in all cases the centers obtained vary by no more than ± 0.3 kHz. The final measured value for the $2\,^3P_1$-to-$2\,^3P_2$ interval is $2\,291\,174.0 \pm 1.4$ kHz.

Table III shows that this is the most precise measurement of $2\,^3P$ fine structure. It disagrees with the previous microwave measurement of Hughes and collaborators [12]. It agrees with the measurements of the groups of Shiner [14] and Minardi [15] and differs by <3 standard deviations from the measurement of Wen and Gabrielse [16], all of whom studied laser $2\,^3S$-to-$2\,^3P$ transitions to measure the interval. The present measurement agrees with the 20-kHz theory of Zhang and Drake [1] and will be a strong test of new QED calculations expected soon [2].

The authors acknowledge the assistance of the Electrical Standards Group at the National Research Council of Canada and support from the Natural Sciences and Engineering Research Council of Canada.

[1] T. Zhang and G. W. F. Drake, Phys. Rev. A **54**, 4882 (1996).
[2] G. W. F. Drake (private communication).
[3] R. S. Van Dyck, Jr., P. B. Schwinberg, and H. G. Dehmelt, Phys. Rev. Lett. **59**, 26 (1987).
[4] T. Kinoshita, IEEE Trans. Instrum. Meas. **46**, 108 (1997).
[5] A. M. Jeffery, R. E. Elmquist, L. H. Lee, J. Q. Shields, and R. F. Dzuiba, IEEE Trans. Instrum. Meas. **46**, 264 (1997).
[6] M. E. Cage *et al.*, IEEE Trans. Instrum. Meas. **38**, 284 (1989).
[7] E. Kruger, W. Nistler, and W. Weirauch, Metrologia **32**, 117 (1995).
[8] Cody Storry, Ph.D. thesis, York University, 1999 (unpublished).
[9] C. H. Storry and E. A. Hessels, Phys. Rev. A **58**, R8 (1998).
[10] W. E. Lamb, Jr., Phys. Rev. **105**, 559 (1957).
[11] Z.-C. Yan and G. W. F. Drake, Phys. Rev. A **50**, R1980 (1994).
[12] F. M. J. Pichanick, R. D. Swift, C. E. Johnson, and V. W. Hughes, Phys. Rev. **169**, 55 (1968); S. A. Lewis, F. M. J. Pichanick, and V. W. Hughes, Phys. Rev. A **2**, 86 (1970); A. Kponou, V. W. Hughes, C. E. Johnson, S. A. Lewis, and F. M. J. Pichanick, Phys. Rev. A **24**, 264 (1981); W. Frieze, E. A. Hinds, V. W. Hughes, and F. M. J. Pichanick, Phys. Rev. A **24**, 279 (1981).
[13] R. F. Clark and A. Jurkus, Rev. Sci. Instrum. **39**, 660 (1968).
[14] D. Shiner, R. Dixson, and P. Zhao, Phys. Rev. Lett. **72**, 1802 (1994); D. L. Shiner and R. Dixson, IEEE Trans. Instrum. Meas. **44**, 518 (1995).
[15] F. Minardi, G. Bianchini, P. Cancio Pastor, G. Giusfredi, F. S. Pavone, and M. Inguscio, Phys. Rev. Lett. **82**, 1112 (1999); P. Cancio, M. Artoni, G. Giusfredi, F. Minardi, F. S. Pavone, and M. Inguscio, in *Atomic Physics 16*, edited by W. E. Baylis and G. W. F. Drake (American Institute of Physics, Woodbury, New York, 1999).
[16] Jesse Wen and G. Gabrielse, Ph.D. thesis, Harvard University, 1996 (unpublished).